Water Solvation Properties: An Experimental and Theoretical Investigation of Salt Solutions at Finite Dilution

3 AUTHORS, INCLUDING:

Roberto Scipioni
University College London
53 PUBLICATIONS **360** CITATIONS

Mauro Boero
Institut de Physique et Chimie des Matéria…
187 PUBLICATIONS **3,473** CITATIONS

Water Solvation Properties: An Experimental and Theoretical Investigation of Salt Solutions at Finite Dilution

Diedrich A. Schmidt,[†,‡] Roberto Scipioni,[†] and Mauro Boero*,[§,||]

International Center for Young Scientists, National Institute for Materials Science, Tsukuba, 305-0044, Japan, Department of Physical Chemistry II, Ruhr-University Bochum, 44780 Bochum, Germany, Institut de Physique et Chimie des Matériaux de Strasbourg, UMR 7504 CNRS-UDS, 23 rue du Loess, BP 43, F-67034 Strasbourg, France, and CREST, Japan Science and Technology Agency, 4-1-8 Honcho, Kawaguchi, Saitama 332-0012, Japan

Our combined analysis of first-principle simulations and experiments conducted on salt solutions at finite dilution shows that the high frequency range of the infrared spectrum of an aqueous solution of NaCl displays a shift toward higher frequencies of the stretching band with respect to pure water. We ascribe this effect to a lowering of the molecular dipole moments due to a decrease in the dipole moments of molecules belonging to the first and second solvation shells with respect to bulk water. An analysis of the dipole orientation correlations proves that the screening of solutes is dominated by short-range effects. These jointly experimental and theoretical results are corroborated by the good agreement between calculated and measured dielectric constants of our target solution.

1. Introduction

The peculiar structural and solvation properties of water have long been understood in terms of a continuous hydrogen-bond (H-bond) network,[1–3] where the H-bond lifetime is on the order of picoseconds.[3–5]

Several experimental approaches have been used to study structural correlations in liquid water,[6–9] and among them, infrared (IR) and Raman spectroscopies also provide additional pieces of information.[10–17]

However, to date, the molecular origin of the stretching band ν_{OH} in the IR spectrum is still a matter of debate. In fact, this band is related to the networked structure of water and hence to the intermolecular coupling due to the H-bonds,[4,18–21] whose effect is to alter the intramolecular O–H bond stretch, thus affecting the dipole moment and, as a direct consequence, the IR and vibrational spectra.[1,17,20–23] Given this scenario, the structure of the stretching band is expected to contain additional information about the H-bond structuring of water. Yet, extracting this important piece of information from the crude data is a nontrivial task and requires additional atomic-level data not directly available from experiments.

In this work, we present a combined theoretical and experimental analysis of the IR stretching band of a NaCl solution at finite dilution, in which the solute density is the one typical of extracellular environments. The results are compared with the ones obtained for pure water to disentangle the effects of the ions from the global behavior of the networked H-bonded water molecules of the bulk solute.

IR spectra are related to the changes of molecular dipole moment inside an H-bond network,[24,25] and thus such a comparison can give important insight into the effects of ions and counterions inside a continuous H-bond network structure. The role of the solvation shells is analyzed in terms of dipole space correlations and shows that the primary effects are mainly restricted to the first hydration shell. These observations have important consequences on the screening effects of water solutions and, as such, are bound to be relevant for hydrophilic interactions of biomolecules.[26]

2. Experimental Details

Experimental IR spectra of highly pure water and analytical grade NaCl solutions were obtained with a BOMEM FT-A2000 MB Fourier transform IR spectrometer in an attenuated total reflection (ATR) configuration using a liquid N_2 cooled HgCdTe (MCT) detector. ATR IR spectroscopy eliminates errors due to saturation and interference effects for small sample volumes.[11–13,15,16,27] Liquid samples (200 μL) were contained in a Teflon cell attached to a Si(001) ATR crystal prism. The experimental setup and solution cell are nearly identical to those used in previous ATR experiments.[28,29] The ATR prisms were $0.5 \times 10 \times 30$ mm with 45° bevels on the 10 mm sides, providing a fixed internal reflection angle of 45°. The design of the liquid cell requires a gasket to seal it, thus reducing the effective length of the Si prism, and because of variations in the size of the Si prism, the resulting number of reflections on the absorbing medium side can vary from 12 to 19 (i.e., 15 on average). Spectra were averaged over 400 scans with a resolution of 4 cm^{-1} at a fixed temperature of 298 K and collected under dry nitrogen gas flow to remove residual water vapor and CO_2. NaCl solutions of 1.18% by mass (0.202 M) were prepared from standard analytical grade NaCl salts and semiconductor grade ultrapure water ($\rho > 18$ MΩ cm). Contact ion pairing was neglected because it has been shown to be negligible at concentrations below ~5 wt % (0.9 M).[30] IR spectra were corrected for both ATR penetration depth dependence[17,27] and density effects.[12,24]

3. Computational Details

First-principle molecular dynamics simulations were performed within the Car–Parrinello framework (CPMD).[31,32]

---

* Corresponding author. E-mail: boero@ipcms.u-strasbg.fr.
† National Institute for Materials Science.
‡ Ruhr-University Bochum.
§ Institut de Physique et Chimie des Matériaux de Strasbourg.
|| Japan Science and Technology Agency.

Valence electrons and atomic positions are treated as dynamical Lagrangean variables evolving simultaneously via Euler−Lagrange equations of motion in which a fictitious electronic mass associated with the electronic degrees of freedom ensures an adiabatic evolution of the electrons and the nuclei.[31] The wave functions of the system are the Kohn−Sham (KS) orbitals, as provided by the density functional theory (DFT).[33] The many-body part of the interaction, referred to as the exchange and correlation functional, was represented by Becke[34] and Lee−Yang−Parr[35] (BLYP) generalized gradient functionals for the exchange and correlation parts, respectively. The core−valence interaction was described by norm-conserving Troullier−Martins pseudopotentials,[36] and KS orbitals were expanded in a plane-waves basis set with a cutoff of 70 Ry in the case of pure water and 80 Ry in the case of Na^+ and Cl^- solutions because of the presence of 2s and 2p semicore states for Na^+. The Brillouin zone of the supercell reciprocal lattice was sampled at the Γ point only, and periodic boundary conditions were applied. The integration time step and the electronic fictitious mass were set to 4.0 au (0.096 fs) and 340.0 au, respectively, to ensure good control of the conserved quantities and of the adiabaticity during the dynamics.[37] A target temperature of 300 K was controlled via a Nosé−Hoover thermostat.[38−40] The fact that the simulation temperature is slightly higher than the experimental temperature is due to the well-known problem of DFT-based simulations, which tend to underestimate the experimental temperature and to give more or less overstructured radial distribution functions, as extensively discussed in the literature.[41] Because the BLYP functional is known to be affected by a slight overbinding leading to a sort of glassy behavior of the dynamics, we performed an auxiliary simulation increasing the temperature to 350 K to check whether the system was trapped in a sort of spurious minimum or not without noticing any changes with respect to the room temperature simulation, as explained in ref 25.

The simulated pure water system consisted of a cubic supercell containing 64 water molecules of side $L = 12.430$ Å (i.e., a density of 1.0 g/cm³), and the simulation lasted for ∼12 ps. We constructed the salt solution first by equilibrating a larger cubic supercell of side $L = 15.644$ Å containing 128 water molecules. After about 10 ps equilibration, two water molecules, separated by ∼9 Å, were replaced by one Na^+ and one Cl^-; amounting to a concentration of ∼0.43 M. We chose this concentration because it is the closest we can get to the experimental concentration considering the size limits on the verge of what is feasible by present-day first-principle approaches of our computational setup. The system was re-equilibrated for 4.0 ps and statistics were collected during the following 19.0 ps. It is important to observe that the simulation times were chosen to allow for meaningful statistics, at least for the part of the IR spectrum we are focusing on. Specifically, we are interested in the stretching part of the spectrum, and a simulation time of 19 ps is sufficiently long to get proper information from the Fourier transform of the dipole−dipole autocorrelation function.[1] Because initial conditions can have an influence in the case of solutes dispersed in a solvent, different starting configurations, with ions at various distances, were considered, and auxiliary CPMD runs were performed for shorter simulation times. However, similar ions tend to stay separated as much as possible, compatibly with the simulation cell size, and we did not find any significant effect with respect to the longer simulation started with the configuration described above.

The total dipole moment was computed at each simulation step to compute the IR spectrum via Fourier transform of the dipole−dipole autocorrelation function. Molecular dipole moments were computed via maximally localized Wannier function centers (WFCs)[42] and uncorrelated configurations extracted from the trajectories of both systems. It has to be mentioned that quantum effects might play a role, as was recently discussed by J. A. Morrone et al.[43] In this work, path integral molecular dynamics (PIMD) was used to compare the results of standard ab initio MD with the case where nuclear quantum effects are included. In some cases, the use of PIMD can worsen rather than improve the agreement with experiments,[44] indicating that other factors such as the degree of accuracy used in the DFT calculation could be more relevant. Moreover, for our purposes, a PIMD approach is beyond the possibility of any present-day computational facility because of the size and time of the simulations performed here.[45] Although quantum vibrations can be corrected from classical trajectory calculations of small systems,[46] this approach would not be suitable for systems with hundreds of atoms. Moreover, even if the vibrational frequencies would be calculated rigorously, calculations of the IR spectra require calculations of dipole moments, hence not just the atomic displacements, and the related dipole−dipole autocorrelation function that are affected by other dominant factors such as the quality of electron wave functions, the accuracy of the DFT functional used, the localization technique used for computing the dipole, and so on. On top of that, we must stress that the presence of solute ions, as will be discussed in the following paragraph, has non-negligible local effects on the water monomers, and the approach used here can take into account these effects in a self-consistent way. Furthermore, it must be underscored that quantum corrections are likely to affect mostly the low-frequency part of the spectrum at room temperature, as shown in ref 1. Indeed, an approach identical to the one used here has also been shown to reproduce the IR spectrum of water accurately under confinement conditions, in which quantum effects are supposed to be even more important.[47] Therefore, we decided to adopt the approach that has been proven to be effective in reproducing water's IR properties.[1,47,48]

4. Results and Discussion

The experimental IR spectrum and the one computed from the simulations upon Fourier transform of the dipole−dipole autocorrelation for pure water and NaCl aqueous solutions turn out to be in pretty good agreement, as shown in Figure 1A. The slight overcorrection of bond lengths, inherent in BLYP gradient-corrected DFT, is responsible for the systematic shift of the theoretical IR curves.[21]

For the sake of clarity, because IR spectra of low-concentration solutions are generally nearly identical to those of pure water, as in this case, they are typically analyzed as difference spectra by subtracting the pure water,[13,15,16] as seen in Figure 1B for experimental and theoretical NaCl solutions of 0.2 and 0.43 M, respectively. Apart from the absolute intensity and known shift due to overcorrection in DFT, key features are well reproduced, that is, the positive (negative) difference peak at higher (lower) wavenumbers. The larger theoretical prediction is attributed to the higher concentration used in calculations. The discrepancy in the lower part of the spectrum, particularly in the H−O−H bending region, although not relevant to the present analysis, can be ascribed to: (i) the presence of the solute that affects the IR spectrum with respect to a pure water system; (ii) the different salt concentrations used in experiments and in simulations; (iii) the need for longer simulation times to

Investigation of Salt Solutions at Finite Dilution

J. Phys. Chem. A, Vol. 113, No. 27, 2009 **7727**
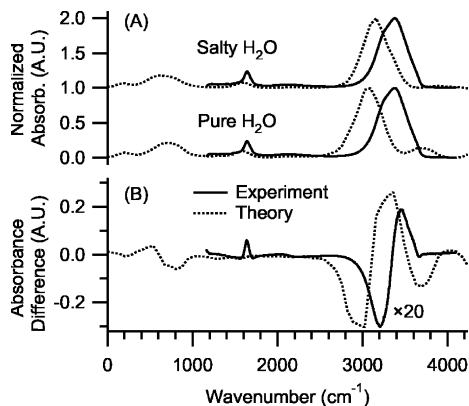
Figure 1. IR spectra of pure and salty water. (A) Experimental and theoretical IR spectra of pure and salty water. Curves offset by 1.0 units for clarity. (B) IR difference spectra; the pure water IR spectra has been subtracted from salty water. Solid and dashed curves are experiment and theory, respectively.
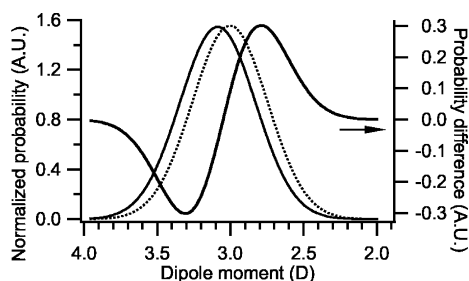
Figure 2. Gaussian distributions of dipole moments for pure (solid) and salty (dashed) water and difference curve (bold) from theory. The distributions are normalized to the area under the curve, and the pure water curve has been subtracted from salty water for the difference curve.

reproduce accurately low frequency bands; and (iv) experimental uncertainties at low frequencies.

In Figure 2, we report the dipole moment distribution for pure water (solid line) and the salt solution (dashed line) computed from the simulations and the difference in the dipole moment distribution (bold, pure water subtracted out). We notice that a clear shift in the distribution of molecular dipole moments appears in the case of the salt solution. Such a shift is in agreement with both experimental and theoretical IR data of Figure 1. Previous investigations have shown an increase in the dipole moment of water from ~1.8 D, typical of gas phase, to a maximum of 2.8 D for water clusters and about 3 D for bulk water.[49,50] The shift to lower molecular dipole moments corresponds to an increase in higher wavenumber contributions in the IR spectra, as seen by a similar qualitative behavior of the curves in Figure 1B. Because water molecules with fewer hydrogen bonds typically have lower dipole moments, we attribute the shifts in IR spectra and molecular dipole moments to an overall lowering of the tetrahedral symmetry in salty water.

The decrease in the molecular dipole moment due to NaCl can be macroscopically seen as a decrease in the static dielectric constant, ε_0, and in the Kirkwood factor

$$G_k = \frac{\langle M^2 \rangle}{N\mu^2} \tag{1}$$

defined as the ratio between the square of the total polarizability, M, and the square molecular dipole, μ, times the number of molecules, N, comprising the system. It is easily understandable
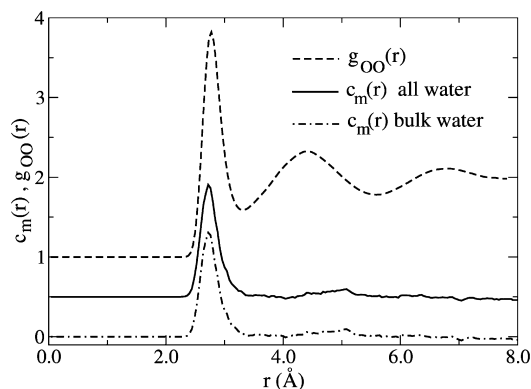
Figure 3. Dipole correlation of H_2O molecules in NaCl solution. The solid line refers to the inclusion of all water molecules, whereas the dotted-dashed line refers to the nonsolvating waters. The dashed upper curve shows the O−O pair correlation for oxygens. Curves are offset 0.5 units along the y axis for clarity.

that for a completely random system with no preferential orientation, $N\mu^2$ is equal to the square average polarizability, and hence $G_k = 1$. In the case of pure water, where a well-structured continuous H-bond network is present, experiment and theory give $G_k = 2.7$[51] and 2.2,[52] respectively. Dielectric relaxation experiments measured $\varepsilon_0 = 72.91$ for 0.404 M NaCl solutions at 298 K.[53] Using the definition of G_k given by eq 1, this means $G_k = 2.5$. A similar analysis on our simulated salt solution (0.43 M) gives a static dielectric constant of 76 ± 6 and $G_k = 2.44$. Both theoretical values for ε_0 and G_k are in good agreement with previous experiments.

To gain deeper insight, we analyzed in more detail the space correlation between ions and water molecules as well as the correlation between different water shells when ions are present in solution. In our previous study, we showed that primarily the first hydration shell is affected by ions, whereas the remaining bulk waters are less affected.[25] To clarify this claim better, we performed a study similar to the one in ref 48, where we computed the spatial dipole−dipole correlation to provide a measure of how far dipole moments are correlated. This can offer precise information on the following points: (i) Does the effect of the ions extend beyond the first or second solvation shell? (ii) Are size effects relevant so that the approximation used in our periodically repeated simulation cell is physically doubtful? To address these issues, we computed the pair dipole correlation $c_m(r)$. Starting from the definition of the dipolar density correlation

$$C_m(r) = \frac{1}{N} \int \langle m(r + r') \cdot m(r') \rangle d^3 r' \tag{2}$$

where

$$m(r) = \sum_{i=1}^{N} \vec{\mu_i}\delta(r - r_i) \tag{3}$$

is the dipolar density, r_i is the position of the ith molecule, and the dipole correlation function $c_m(r)$ is defined as

$$c_m(r) = \frac{1}{\rho}(C_m(r) - \langle \mu^2 \rangle\delta(r)) \tag{4}$$
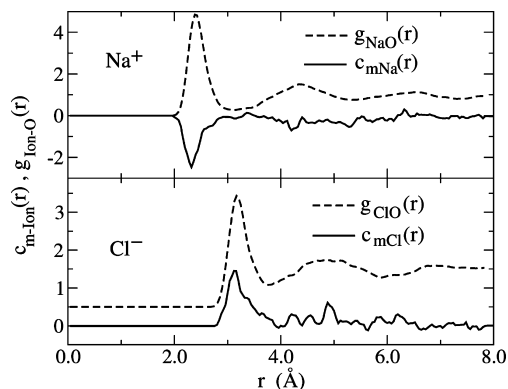
Figure 4. Water molecular dipole correlations with Na^+ and Cl^-. The upper panel shows the $Na-O$ pair correlation (dashed line) and the ion–dipole correlation (solid line). The lower panel shows the $Cl-O$ pair correlation (dashed line) and the ion–dipole correlation (solid line).

where ρ is the molecular density. Figure 3 shows the results for the entire solvent and water molecules not belonging to the ion's first hydration shell, respectively.

Interestingly, both curves show a pronounced peak around 2.7 to 2.8 Å, which is due to the alignment of adjacent dipoles via H bonds. Although a small peak is visible around 5.0 Å, most of the alignment occurs in the range between 2.5 and 3.3 Å and is a consequence of the standard tetrahedral network of H-bonded molecules; for comparison, the upper curve shows the $g_{OO}(r)$ pair correlation function for the oxygens. The decay of the dipole correlation beyond ∼5.5 Å (second coordination shell) is an indication that water molecules beyond these distances are not dipole-correlated with each other, which is in agreement with ref 52. The negligible long-range dipolar correlation also implies that size effects are minimal here.

We also calculated the ion–dipole correlation for both Na^+ and Cl^-. In this case, the ion–dipole correlation is defined using the same formula as that reported in eq 2 with $\langle \mathbf{m}(\mathbf{r} + \mathbf{r'}) \cdot \mathbf{m}(\mathbf{r'}) \rangle$ replaced by $\langle \mathbf{m}(\mathbf{r} + \mathbf{r'}) \cdot \mathbf{r'} \rangle$, where $\mathbf{r'}$ is the position of either the cation Na^+ or the anion Cl^-. This quantity gives an indication of the space correlations of the molecular dipoles oriented in shells around the ions. The results are summarized in Figure 4.

Although some additional small alignment occurs at distances around 4.5 to 5.5 Å, in particular, in the case of the larger anion Cl^-, the first hydration shell is primarily responsible for most of the orientation. Beyond these distances, the water molecule dipoles appear to be uncorrelated and largely unaffected by the presence of the ions. Therefore, the rest of the solvent behaves like bulk water because screening effects are already achieved at distances around 5.5 Å. This has practical importance in several cases where solvating water molecules are present in limited amounts; for instance, in biosystems such as proteins or nucleic acids, where a few H_2O molecules can be trapped in pockets or folded structures, together with counterions.

5. Conclusions

In conclusion, experiments and simulations show that salt ions modify the IR properties of water as a consequence of changes in the distribution the molecular dipole moments of the solution. Both theory and experiments indicate a lowering of dipole moments; this lowering is partially due to the molecules in the first and second solvation shells not being polarized to the extent of water molecules in bulk water. As shown in previous studies[48,52] and confirmed here, the dipole orientation correlation of molecules outside the first two solvation shells is largely unaffected by the ions, therefore indicating that screening effects even work at short distances. This has important consequences in biomolecular systems where hydration radii can range from 5 to 18 Å.[54,55] The negligible dipole correlation found beyond 5 Å indicates that size effects are not relevant in this case and are not responsible for the effects observed. This is corroborated by the agreement of the dielectric constant of NaCl calculated from our simulations and that reported for previous experiments on analogous solutions and from the complementary information provided by our experiments.

References and Notes

(1) Silvestrelli, P. L.; Bernasconi, M.; Parrinello, M. *Chem. Phys. Lett.* **1997**, *277*, 478–482.
(2) Rull, F. *Pure Appl. Chem.* **2002**, *74*, 1859–1870.
(3) Matsumoto, M.; Baba, A.; Ohmine, I. J. *J. Chem. Phys.* **2007**, *127*, 134504.
(4) Eaves, J. D.; Loparo, J. J.; Fecko, C. J.; Roberts, S. T.; Tokmakoff, A.; Geissler, P. L. *Proc. Natl. Acad. Sci. U.S.A.* **2005**, *102*, 13019–13022.
(5) Boero, M.; Terakura, K.; Ikeshoji, T.; Liew, C. C.; Parrinello, M. *Phys. Rev. Lett.* **2000**, *85*, 3245–3248.
(6) Soper, A. K.; Bruni, F.; Ricci, M. A. *J. Chem. Phys.* **1997**, *106*, 247–254.
(7) Wernet, Ph.; Nordlund, D.; Bergmann, U.; Cavallieri, M.; Odelius, M.; Ogasawara, H.; Näslund, L. Å.; Hirsch, T. K.; Ojamäe, L.; Glatzel, P.; Pettersson, L. G. M.; Nilsson, A. *Science* **2004**, *304*, 995.
(8) Smith, J. D.; Cappa, C. D.; Wilson, K. R.; Messer, B. M.; Cohen, R. C.; Saykally, R. J. *Science* **2004**, *306*, 851–853.
(9) Winter, B.; Aziz, E. F.; Hergenhahn, U.; Faubel, M.; Hertel, I. V. *J. Chem. Phys.* **2007**, *126*, 124504.
(10) Walrafen, G. E. *J. Chem. Phys.* **1970**, *52*, 4176–4198.
(11) Bertie, J. E.; Ahmed, M. K.; Eysel, H. H. *J. Phys. Chem.* **1989**, *93*, 2210–2218.
(12) Max, J. J.; Trudel, M.; Chapados, C. *Appl. Spectrosc.* **1998**, *52*, 234–239.
(13) Max, J. J.; Chapados, C. *J. Chem. Phys.* **2000**, *113*, 6803–6814.
(14) Walrafen, G. E.; Pugh, E. *J. Solution Chem.* **2004**, *33*, 81–97.
(15) Chen, Y.; Zhang, Y.-H.; Zhao, L.-J. *Phys. Chem. Chem. Phys.* **2004**, *6*, 537–542.
(16) Wei, Z.-F.; Zhang, Y.-H.; Zhao, L.-J.; Liu, J.-H.; Li, X.-H. *J. Chem. Phys. A* **2005**, *109*, 1337–1342.
(17) Schmidt, D. A.; Miki, K. *J. Phys. Chem. A* **2007**, *111*, 10119–10122.
(18) Coker, D. F.; Miller, R. E.; Watts, R. O. *J. Chem. Phys.* **1985**, *82*, 3554–3562.
(19) Sceats, M. G.; Stavola, M.; Rice, S. A. *J. Chem. Phys.* **1979**, *71*, 983–990.
(20) Schofield, D. P.; Lane, J. R.; Kjaergaard, H. G. *J. Phys. Chem. A* **2007**, *111*, 567–572.
(21) Chen, W.; Sharma, M.; Resta, R.; Car, R. *Phys. Rev. B* **2008**, *77*, 245114.
(22) Goldman, N.; Saykally, R. J. *J. Chem. Phys.* **2004**, *120*, 4777–4789.
(23) Ohno, K.; Okimura, M.; Akai, N.; Katsumoto, Y. *Phys. Chem. Chem. Phys.* **2005**, *7*, 3005–3014.
(24) Schmidt, D. A.; Miki, K. *ChemPhysChem* **2008**, *9*, 1914–1919.
(25) Scipioni, R.; Schmidt, D. A.; Boero, M. *J. Chem. Phys.* **2009**, *130*, 024502.
(26) Ebbinghaus, S.; Kim, S. J.; Heyden, M.; Yu, X.; Heugen, U.; Gruebele, M.; Leitner, D. M.; Havenith, M. *Proc. Natl. Acad. Sci. U.S.A.* **2007**, *104*, 20749–20752.
(27) Harrick, N. J. *Internal Reflection Spectroscopy*; John Wiley & Sons: New York, 1967.
(28) Kimura, Y.; Nemoto, J.; Shinohara, M.; Niwano, M. *Phys. Status Solidi A* **2003**, *197*, 577–581.
(29) Miyamoto, K.; Ishibashi, K.; Yamaguchi, R.-T.; Kimura, Y.; Ishii, H. *J. Appl. Phys.* **2006**, *99*, 094702.
(30) Mancinelli, R. J.; Botti, A.; Bruni, F.; Ricci, M. A. *Phys. Chem. B* **2007**, *111*, 13570–13577.

Investigation of Salt Solutions at Finite Dilution

J. Phys. Chem. A, Vol. 113, No. 27, 2009 **7729**

(31) Car, R.; Parrinello, M. *Phys. Rev. Lett.* **1985**, *55*, 2471–2474.

(32) *CPMD Code*; Copyright IBM Corp., 1990−2001; Copyright MPI für Festkörperforschung, Stuttgart, 1997−2004. http://www.cpmd.org.

(33) Kohn, W.; Sham, L. J. *Phys. Rev.* **1965**, *140*, A1133−A1138.

(34) Becke, A. D. *Phys. Rev. A* **1988**, *38*, 3098–3100.

(35) Lee, C.; Yang, W.; Parr, R. G. *Phys. Rev. B* **1988**, *37*, 785–789.

(36) Troullier, N.; Martins, J. L. *Phys. Rev. B* **1991**, *43*, 1993–2006.

(37) Schwegler, E.; Grossman, J. C.; Gygi, F.; Galli, G. *J. Chem. Phys.* **2004**, *121*, 5400–5409.

(38) Nosé, S. *Mol. Phys.* **1984**, *52*, 255–268.

(39) Nosé, S. *J. Chem. Phys.* **1984**, *81*, 511–519.

(40) Hoover, W. G. *Phys. Rev. A* **1985**, *31*, 1695–1697.

(41) Boese, A. D.; Doltsinis, N. L.; Handy, N. C.; Sprik, M. *J. Chem. Phys.* **2000**, *112*, 1670–1678.

(42) Marzari, N.; Vanderbilt, D. *Phys. Rev. B* **1997**, *56*, 12847–12865.

(43) Morrone, J. A.; Car, R. *Phys. Rev. Lett.* **2008**, *101*, 017801.

(44) Mantz, Y. A.; Chen, B.; Martyna, G. J. *J. Phys. Chem B* **2006**, *110*, 3540–3554.

(45) Mei, S. H.; Tuckerman, M. E.; Sagnella, D. E.; Klein, M. L. *J. Phys. Chem. B* **1998**, *102*, 10446–10458.

(46) Yamada, T.; Aida, M. *Chem. Phys. Lett.* **2008**, *452*, 315–320.

(47) Sharma, M.; Donadio, D.; Schwegler, E.; Galli, G. *Nano Lett.* **2008**, *8*, 2959–2962.

(48) Chen, W.; Sharma, M.; Resta, R.; Galli, G.; Car, R. *Phys. Rev. B* **2008**, *77*, 245114.

(49) Gregory, J. K.; Clary, D. C.; Liu, K.; Brown, M. G.; Saykally, R. J. *Science* **1997**, *275*, 814–817.

(50) Coudert, F.-X.; Vuilleumier, R.; Boutin, A. *ChemPhysChem* **2006**, *7*, 2464–2467.

(51) Buchner, R.; Barthel, J.; Stauber, J. *Chem. Phys. Lett.* **1999**, *306*, 57–63.

(52) Sharma, M.; Resta, R.; Car, R. *Phys. Rev. Lett.* **2007**, *98*, 247401.

(53) Buchner, R.; Hefter, G. T.; May, P. M. *J. Phys. Chem. A* **1999**, *103*, 1–9.

(54) Heugen, U.; Schwaab, G.; Bründemann, E.; Heyden, M.; Yu, X.; Leitner, D. M.; Havenith, M. *Proc. Natl. Acad. Sci. U.S.A.* **2006**, *103*, 12301–12306.

(55) Born, B.; Kim, S. J.; Ebbinghaus, S.; Gruebele, M.; Havenith, M. *Faraday Discuss.* **2009**, *141*, 161–173.